

Stiffness loss of laminates with aligned intralaminar cracks Part II. Comparisons

T. LEWIŃSKI and J.J. TELEGA (WARSAWA)

THE EFFECTIVE MODELS (h_0, l_0) and (h_0, l) [7] describing reduction of the in-plane effective moduli of the $[0_m^\circ/90_n^\circ]_s$ cross-ply composites cracked in the internal layer and subjected to in-plane boundary forces are applied to the description of the degradation of the effective Young, Kirchhoff and Poisson moduli of the $[0^\circ/90^\circ]_s$ and $[0^\circ/90_3]_s$ glass/epoxy and $[0^\circ/90_2]_s$ graphite/epoxy laminates. It is shown that the graphs of $E_1(c_d)$ (c_d represents crack density) lie slightly above the Hashin's curves, while $G_{12}(c_d)$ predictions coincide with the curves of Hashin. Evaluation of the off-diagonal terms, i.e. $\nu_{12}(c_d)$, $\nu_{21}(c_d)$ are incorporated in the algorithm. In all comparisons with the experimental results of Groves, Ogin, Highsmith and Reifsnider the predictions of $E_1(c_d)$ according to the model (h_0, l) provide lower bounds, slightly better than the bounds of Hashin. Some predictions of the model (h_0, l) are proved to be similar to McCartney's "generalized-plane-strain" results.

1. Introduction

THE FIRST DAMAGE mode observed in the in-plane loaded, three-layer, balanced cross-ply laminates is usually transverse cracking along the fibres of the outer or inner layers. When stretched along the fibres of the outer layers or sheared in its plane, samples of the balanced $[0_m^\circ/90_n^\circ]_s$ laminates undergo transverse cracking in the 90° layer, with values of crack density c_d determined by magnitude of the in-plane loads applied. Such cracks lead to degradation of effective elastic characteristics of the laminate. A unified model of such degradation has recently been proposed in Refs. [I.9, I.10] (Roman numeral I refers to bibliography of the first part of this paper, [7]) and in Ref. [7], where the case of aligned cracks is dealt with in detail. The aim of this paper is twofold. First we show that the (h_0, l_0) model (Ref. [I.10], Sec. 4) concerns the case of infinitely dense distribution of cracks. Consequently, this model provides the asymptotes for the curves of decay of the effective moduli with respect to the crack density. Then we check the accuracy of the (h_0, l) model proposed in Ref. [I.10]. To assess its accuracy with respect to the experimental results published in the available literature, we analyze the decay of:

- the effective Young modulus E_1^c of laminates of the $[0_m^\circ/90_n^\circ]_s$ type. Accuracy of the (h_0, l) predictions is examined for the laminates tested by GROVES [I.4] (cf. LEE *et al.* [6]), HIGHSMITH and REIFSNIDER [I.6] and by OGIN *et al.* [9];
- the effective moduli of Kirchhoff (G_{12}^c), Young (E_2^c) and Poisson ($\nu_{\alpha\beta}^c$) for the $[0^\circ/90_3]_s$ laminate tested by HIGHSMITH and REIFSNIDER [I.6].

The results concerning E_1^c show that the (h_0, l) method leads to lower estimates of the experimental data, providing the curves lying closer to the test data than the

curves produced by the method of HASHIN [I.5] and almost coinciding with recent McCARTNEY's [I.12, I.13] GPS (generalized plane strain model) – predictions.

The formula for G_{12}^c coincides with that found by HASHIN [I.5] and rederived later by TAN and NUISMER [I.14] and TSAI and DANIEL [I.16]. According to the experimental results published in the last paper, concerning the graphite/epoxy $[0^\circ/90_2^\circ]_s$ and $[0^\circ/90_4^\circ]_s$ laminates, the accuracy of this formula is satisfactory. On the other hand, the experiments concerning graphite/epoxy AS/3502 ($0_2^\circ/90_2^\circ$) laminates performed by HAN and HAHN [4] do not confirm its utility, cf. their paper and the discussion by MOTOGI and FUKUDA [8].

Our analysis shows that predictions of the (h_0, l_0) model proposed in Ref. [I.10] are comparable with the ply-discount method.

The (h_0, l) method predicts a small decay of the E_2^c modulus of the $[0^\circ/90_3^\circ]_s$ glass/epoxy laminates, very similar to that predicted by the GPS model of McCARTNEY [I.13]. Other methods known to the present authors do not describe the decay of E_2^c or keep an open mind on the subject.

The (h_0, l) method provides a unified algorithm for predicting decay of all components of the stiffness matrix. In particular, the method makes it possible to evaluate the decay of Poisson ratios. In the present paper the curves of the decay of these ratios for the glass/epoxy $[0^\circ/90_3^\circ]_s$ laminate are given and compared with GPS-predictions of McCARTNEY [I.13]. A very close juxtaposition of these predictions are noted. For the laminate analyzed no relevant experimental results were available to us. The only experimental results available to the present authors, concerning reduction of Poisson ratios of other types of laminates, are given in SMITH and WOOD [10]. A comparison of these results with (h_0, l) predictions will be published separately. The present paper concerns only the case of cracking in the internal layer. A generalization to the case of the simultaneous cracking in external and internal layers requires a reformulation of the original model of Sec. 2 proposed by LEWIŃSKI and TELEGA [I.9], which could probably be done by adopting the assumptions put forward by HASHIN [5] and TSAI and DANIEL [I.16].

The system of notations is compatible with that employed in Part I of the present paper, namely in Ref. [7]. For the sake of brevity, Roman numeral I refers also to equations or sections of Part I.

2. Parallel cracks. Comparison of (h_0, l_0) and (h_0, l) predictions

The subject of consideration will be the same as in Ref. [7], Secs. 3, 4. We examine a three-layer laminate of thickness $2h$ weakened by regularly distributed transverse cracks in the internal layer, and subject to in-plane loading; the crack spacing equals l , cf. Fig. I.2. These cracks result in the degradation of effective moduli. The aim of this section is to prove that decaying curves of moduli degradation predicted by the (h_0, l) model presented in Ref. [7], Sec. 4, tend to crack density-independent values of the effective moduli, predicted by the (h_0, l_0) model

proposed in Sec.3 of [7], if the number of cracks tends to infinity.

2.1. Stiffnesses $\tilde{A}_c^{\alpha\alpha\beta\beta}$ versus $A_c^{\alpha\alpha\beta\beta}$

Let us compare formulae (I.3.9) with (I.4.26) and (I.3.13) with (I.4.27). Note that the line of non-smoothness of the constitutive relations: $E_h = 0$ is common for both approaches, which makes the results of both approaches similar. However, Eq. (I.3.10) is independent of $\varrho = l/2h$. Let us examine the $\tilde{A}_c^{\alpha\alpha\beta\beta}(\varrho)$ curves.

If ϱ tends to infinity, $F_{11}(\varrho)$ tends to zero. Hence

$$(2.1) \quad \lim_{\varrho \rightarrow \infty} \tilde{A}_c^{\alpha\alpha\beta\beta} = A_1^{\alpha\alpha\beta\beta}.$$

Thus if the crack spacing is much greater than h , the loss of stiffness will not be observed. This effect is also observed in experiments, which will be discussed in Sec.3. According to the (h_0, l_0) model, the loss of stiffness is ϱ -independent provided that ϱ is small, cf. comments in Ref. [I.10].

Consider the case when the number of cracks increases to infinity; then $\varrho \rightarrow 0$. One can prove that

$$(2.2) \quad \begin{aligned} \lim_{\varrho \rightarrow 0} F_0(\varrho; \omega, \sigma) &= \frac{1}{\sigma^2 \omega^2}, \\ \lim_{\varrho \rightarrow 0} F_0(\varrho; \omega, \sigma) &= \frac{1}{(p^2 + q^2)^2}. \end{aligned}$$

Since $\sigma^2 \omega^2 = (p^2 + q^2)^2$, we see that both limits coincide, irrespective of whether the roots of polynomial (I.4.13) are real or complex. Hence we have

$$(2.3) \quad \lim_{\varrho \rightarrow 0} (\tilde{\varepsilon}_{11}^F / E_h) = F_{11}(0),$$

for the case $E_h > 0$, where $F_{11}(0) = \lim_{\varrho \rightarrow 0} F_{11}(\varrho)$ is given by

$$(2.4) \quad F_{11}(0) = a_3 f_{11} [(\beta_{11} \gamma_{11} + \gamma_{21}) a_1 - (\beta_{11} \gamma_{13} + \gamma_{23}) a_2 + (\beta_{11} \gamma_{12} + \gamma_{22}) a_3]^{-1}.$$

On the other hand, according to the (h_0, l_0) approach, for the case $E_h > 0$ one finds

$$(2.5) \quad \varepsilon_{11}^F / E_h = F_{11}^0,$$

F_{11}^0 being defined by Eq. (I.3.8)₁. By using the relations between constants summarized in the Appendix of [7], after lengthy algebraic calculations one can prove that $F_{11}(0) = F_{11}^0$, which confirms the thesis of Sec.5.6 of Ref. [I.10]: the (h_0, l_0) model provides asymptotes for the curves predicted by the (h_0, l) model, namely

$$(2.6) \quad \lim_{\varrho \rightarrow 0} \tilde{A}_c^{\alpha\alpha\beta\beta} = A_c^{\alpha\alpha\beta\beta}.$$

2.2. Stiffness \tilde{A}_c^{1212} versus A_c^{1212}

One can prove that

$$(2.7) \quad \lim_{\varrho \rightarrow 0} F_{12}(\hat{\lambda}\varrho) = \frac{c}{h}, \quad \lim_{\varrho \rightarrow \infty} F_{12}(\hat{\lambda}\varrho) = 0,$$

and hence, cf. Eq. (I.3.21)

$$(2.8) \quad \lim_{\varrho \rightarrow 0} \tilde{\varepsilon}_{12}^F = \varepsilon_{12}^F, \quad \lim_{\varrho \rightarrow 0} \tilde{A}_c^{1212} = A_c^{1212},$$

$$(2.9) \quad \lim_{\varrho \rightarrow \infty} \tilde{A}_c^{1212} = A_v^{1212}.$$

Thus, if the crack density ϱ^{-1} tends to zero, the stiffness \tilde{A}_c^{1212} tends to the stiffness A_v^{1212} of the uncracked laminate. If the crack density tends to infinity, the (h_0, l) predictions tend to (h_0, l_0) predictions (I.3.21)–(I.3.23). In particular, a constant line $G_{12}^c = A_c^{1212}/2h$ is an asymptote for the \tilde{G}_{12}^c curve describing the decays of the effective Kirchhoff modulus.

We observe that (2.6) and (2.9) imply the relation between hyperelastic potentials

$$(2.10) \quad \mathcal{V}_h = \lim_{\varrho \rightarrow 0} W_h(\varrho).$$

The line of non-smoothness of both potentials $E_h = 0$ remains ϱ -independent.

3. Degradation of effective stiffnesses of laminates $[0_n^\circ/90_m^\circ]_s$. Comparison with experimental results and with other analytical predictions

In this section we shall verify the (h_0, l_0) and (h_0, l) models predictions for:

i) $[0_n^\circ/90_m^\circ]_s$ glass/epoxy laminates tested by HIGHSMITH and REIFSNIDER [I.6] and by OGIN *et al.* [9].

ii) $[0^\circ/90_2^\circ]_s$ graphite/epoxy laminates tested by GROVES [I.4] (this paper was not available for the present authors; Groves' results are reported here after LEE *et al.* [6]).

The results of Sec. I.4 will be compared with theoretical predictions of ABOUDI [1], HASHIN [I.5] and LEE *et al.* [6].

3.1. $[0^\circ/90_3^\circ]_s$ glass/epoxy laminate

We start with the laminate first examined by HIGHSMITH and REIFSNIDER [I.6] and then often referred to in the relevant literature. The complete characteristics of this laminate have been recorded by HASHIN [I.5, Sec. 4]. We repeat them to make our paper self-contained. The external plies are 0° -plies, their thickness d being equal to 0.203 mm; the internal layer composed of 90° -plies has thickness

$2c, c = 3d$, cf. Fig. I.2. The compliances $D_{ijkl}^{\mathbf{n}}$ ($\mathbf{n} = m, f$) cf. Eq. (2.3) of Ref. [I.9] are defined by

$$(3.1) \quad \begin{aligned} D_{1111}^f &= D_{2222}^m = \frac{1}{E_A}, & D_{1111}^m &= D_{2222}^f = D_{3333}^f = D_{3333}^m = \frac{1}{E_T}, \\ D_{1122}^f &= D_{1122}^m = D_{1133}^f = D_{2233}^m = -\frac{\nu_A}{E_A}, \\ D_{1133}^m &= D_{2233}^f = -\frac{\nu_T}{E_T}, \\ D_{1212}^f &= D_{1212}^m = D_{2323}^m = \frac{1}{4G_A}, \\ D_{1313}^f &= \frac{1}{4G_A}, & D_{1313}^m &= D_{2323}^f = \frac{1}{4G_T}, \end{aligned}$$

where, according to Table 1 of HASHIN [I.5],

$$(3.2) \quad \begin{aligned} E_A &= 41.7 \text{ GPa}, & E_T &= 13.0 \text{ GPa}, & G_A &= 3.4 \text{ GPa}, \\ G_T &= 4.58 \text{ GPa}, & \nu_A &= 0.30, & \nu_T &= 0.42. \end{aligned}$$

The index A labels the fibre direction, while T indicates the direction transverse to the fibres.

Now we can determine the generalized compliances $\mathbf{D}^N, \mathbf{D}^L, \mathbf{D}^{NL}, \mathbf{D}^Q, \mathbf{D}^{RL}, \mathbf{D}^{RN}, D^R$ by Eqs. (2.17) of Ref. [I.9]. Then we invert the constitutive matrices of Eqs. (2.19) and (2.20) of Ref. [I.9] and find the stiffness matrices of the primal constitutive relationships (2.24) and (2.25) of [I.9]. We can calculate the stiffnesses (4.9) of Ref. [I.10] and then the effective moduli (I.3.16) of the uncracked laminate. We obtain

$$(3.3) \quad \begin{aligned} E_1 &= 20.30 \text{ GPa}, & E_2 &= 34.75 \text{ GPa}, & G_{12} &= 3.40 \text{ GPa}, \\ \nu_{12} &= 0.193, & \nu_{21} &= 0.113. \end{aligned}$$

The first three results coincide with the data reported by HASHIN [I.5], while results concerning E_α and $\nu_{\alpha\beta}$ coincide with those obtained by MCCARTNEY ([I.12], Appendix A).

According to the in-plane scaling ((h_0, l_0) approach), the reduced moduli are crack density independent. Using formulae (I.3.13) and (I.3.16) for the case of $\nu_{\alpha\beta}^c, E_\alpha^c$, and (I.3.23)₂, (I.3.22)₂ we find

$$(3.4) \quad \begin{aligned} E_1^c &= 10.70 \text{ GPa}, & E_2^c &= 34.53 \text{ GPa}, & G_{12}^c &= 0.85 \text{ GPa}, \\ \nu_{12}^c &= 0.0943, & \nu_{21}^c &= 0.0292. \end{aligned}$$

According to the experimental data of HIGHSMITH and REIFSNIDER [I.6], the minimum value of E_1^c achieved for 0.75 cracks/mm equals 11.0 GPa while $E_1 =$

21.0 GPa. However, it is not sure whether the values measured in the paper cited above are viewed as the effective Young moduli or have been defined by means of the longitudinal stiffnesses

$$\bar{E}_1 = A_1^{1111}/2h, \quad \bar{E}_1^c = A_c^{1111}/2h.$$

It is worth noting that the results $\bar{E}_1 = 20.76$ GPa, $\bar{E}_1^c = 10.73$ GPa lie closer to the values found experimentally than the quantities E_1, E_1^c which are Young moduli by the definition.

The experiments show that the reduction of the effective characteristics depends upon the crack density. The space-scaling (h_0, l) approach accounts for such a dependence. Having found the matrices involved in Eqs. (3.16) of [I.10] one can calculate the parameters defined by Eqs. (I.A.1)–(I.A.4) and then the coefficients of Eq. (I.4.13). The roots of this characteristic equation turn out to be complex $(p, \pm q)$, where $p = 1.98025$ and $q = 0.8934$, hence the function $F_{11}(\varrho)$ is defined by means of $F = F_0$, cf. Eqs. (I.4.23) and (I.4.24). The decay of stiffnesses is defined by (I.4.27) and (I.4.43)₂. The effective Young, Poisson and Kirchhoff moduli are given by Eqs. (I.4.29) and (I.4.44).

As it has been emphasized by LEE *et al.* [6], the decay of the stiffnesses should rather be displayed versus the crack density defined by $2c/l$ (crack depth/crack spacing). However, to compare our results with the theoretical predictions of HASHIN [I.5] and with experimental data of HIGHSMITH and REIFSNIDER [I.6], we quote them in some of our figures also as functions of the crack density c_d defined as 1 mm/l.

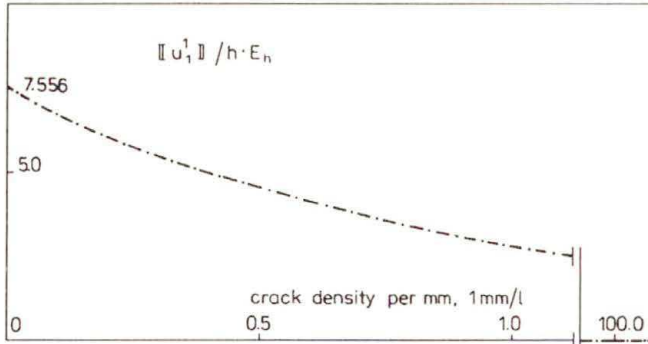


FIG. 1. $[0^\circ/90_3^\circ]_s$ glass/epoxy laminate tested by HIGHSMITH and REIFSNIDER [I.6]. The crack opening $[[u_1^\varepsilon/h_\varepsilon]] = [[u_1^1/h]]$ (normalized with respect to E_n) versus crack density.

The crack opening $[[u_1^\varepsilon/h_\varepsilon]] = [[u_1^1/h]] + 0(\varepsilon)$ decays to zero if c_d tends to infinity, cf. Fig. 1. The longitudinal crack deformation $\tilde{\varepsilon}_{11}^F$ behaves quite differently. The curve $\tilde{\varepsilon}_{11}^F(c_d)$ starts from zero and tends asymptotically to the ε_{11}^F value predicted by the in-plane scaling method (h_0, l_0) , cf. Fig. 2. The shear crack deformation $\tilde{\varepsilon}_{12}^F$ behaves similarly, cf. Fig. 3. For sufficiently large values of c_d the

crack deformations $\tilde{\epsilon}_{11}^F, \tilde{\epsilon}_{12}^F$ become practically independent of the crack density. This insensibility to large values of c_d corresponds to the saturation of cracks observed in experiments, cf. GARRETT and BAILEY [I.2].

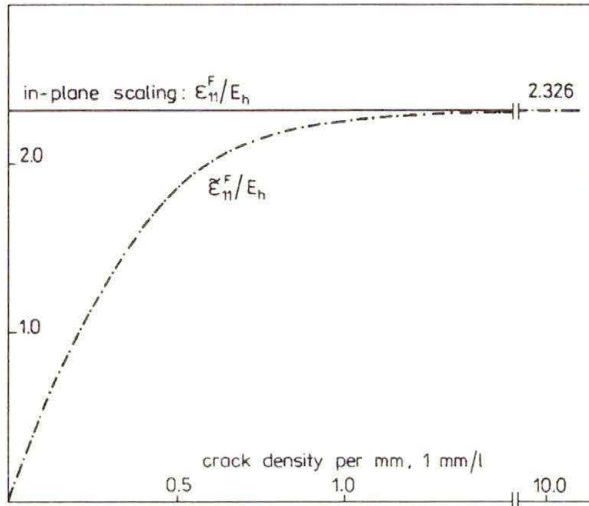


FIG. 2. The same laminate. Longitudinal crack deformation versus crack density. The in-plane scaling prediction: $\epsilon_{11}^F \approx \epsilon_{11}^h + 0.299\epsilon_{22}^h$ is an asymptote for the space scale prediction $\tilde{\epsilon}_{11}^F$.

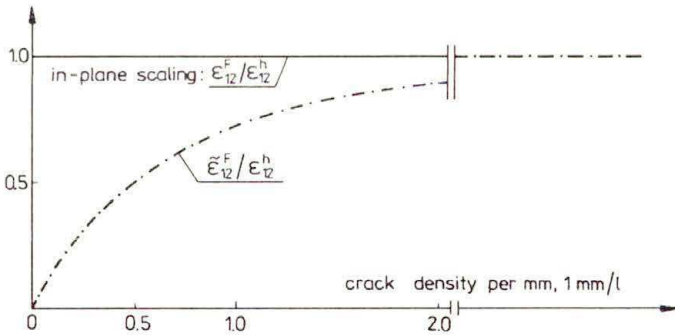


FIG. 3. The same laminate. Shear crack deformation versus crack density. The in-plane scaling prediction $\epsilon_{12}^F = \epsilon_{12}^h$ is an asymptote for the space scaling prediction $\tilde{\epsilon}_{12}^F$.

The decay of the effective Young modulus \tilde{E}_1^c observed in experiments by HIGHSMITH and REIFSNIDER [I.6] and predicted by the method of HASHIN [I.5], the GPS method of McCARTNEY [I.12], the method of LEE *et al.* [6], cf. ALLEN *et al.* [2], and by the space-scaling based (h_0, l) method is presented in Fig. 4. The Hashin's curve has not been repeated after Fig. 3 in HASHIN [I.5] but has been independently plotted by the present authors. The experimental data are placed according to Fig. 14 in HIGHSMITH and REIFSNIDER [I.6] and Fig. 1a in LEE

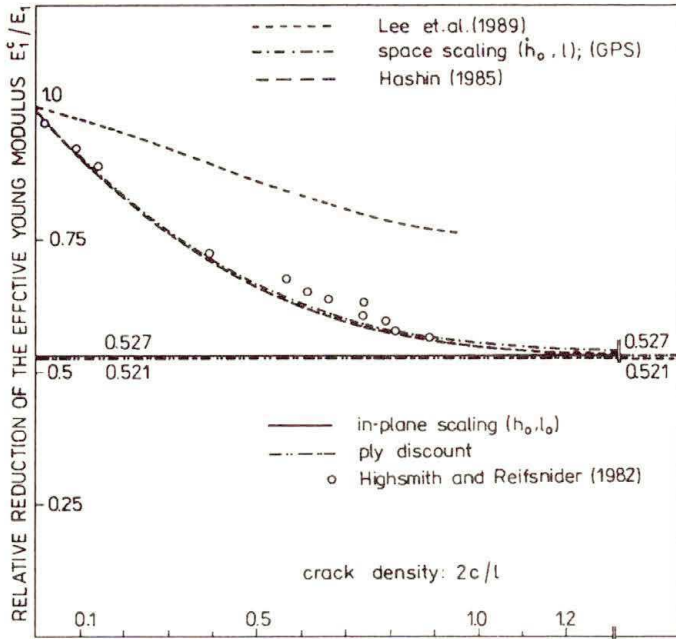


FIG. 4. The same laminate. Assessing the loss of the effective Young modulus E_1 versus crack density. Experimental results of HIGHSMITH and REIFSNIDER [1.6] are denoted by circles.

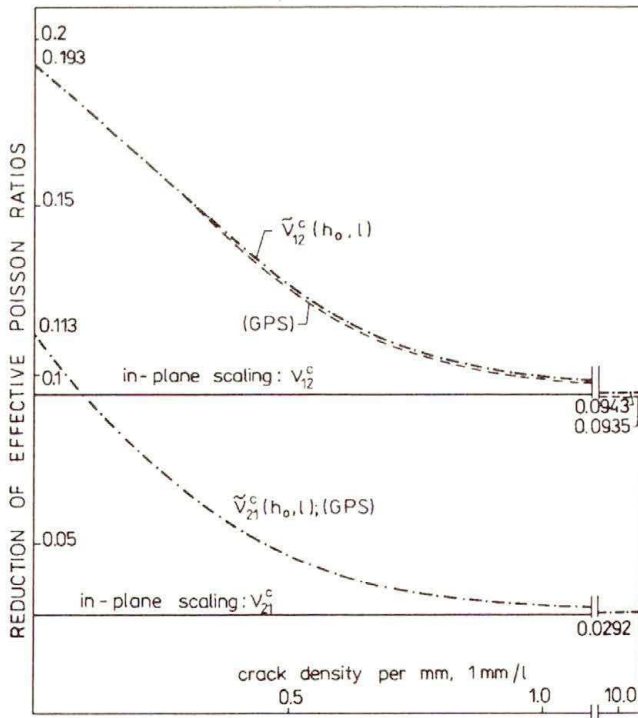


FIG. 5. The same laminate. Effective Poisson ratios as functions of the crack density.

et al. [6]. The Hashin's curve lies slightly below the curves predicted by the GPS model and by the (h_0, l) space-scaling method, the juxtaposition of the last two curves being too close to be noticeable in Fig. 4. The curves mentioned above provide lower bounds for the experimental results. Small differences in these results can be read off from Table 1a. On the other hand, the predictions of LEE *et al.* [6] are upper bounds for the experimental data. The in-plane scaling method $((h_0, l_0)$ approach) determines a horizontal asymptote for the \tilde{E}_1^c/E_1 curve; the conventional ply-discount assessment lies a little below and is an asymptote for the Hashin's curve.

Table 1. Decay of E_α^c/E_α , $\nu_{\alpha\beta}^c$ as function of crack density $2c/l$ for the $(0^\circ/90_3^\circ)_s$ glass/epoxy laminate tested by HIGHSMITH and REIFSNIDER (1982). Comparison of predictions by (h_0, l) model proposed with results due to HASHIN (1985) (case E_1^c/E_1) and model (GPS) of McCARTNEY (1992, 1993).

(a)				(c)		
$2c/l$	E_1^c/E_1			$2c/l$	ν_{21}^c	
	Hashin (1985)	McCartney (1992) GPS	Lewiński and Telega (h_0, l)		McCartney (1992) GPS	Lewiński and Telega (h_0, l)
0.1	0.9069	0.90918	0.90914	0.1	0.09684	0.09688
0.5	0.6609	0.66638	0.66628	0.5	0.05375	0.05390
1.0	0.54782	0.55347	0.55341	1.0	0.03371	0.03393
100.	0.52127	0.52683	0.52681	100.	0.0290	0.02922

(b)			(d)		
$2c/l$	ν_{12}^c		$2c/l$	E_2^c/E_2	
	McCartney (1992) GPS	Lewiński and Telega (h_0, l)		McCartney (1992) GPS	Lewiński and Telega (h_0, l)
0.1	0.18215	0.18223	0.1	0.99929	0.99930
0.5	0.13753	0.1380	0.5	0.99644	0.99650
1.0	0.10362	0.10432	1.0	0.99428	0.99437
100.	0.09353	0.09432	100.	0.99364	0.99374

The decaying character of the graphs $\tilde{\nu}_{12}^c$, $\tilde{\nu}_{21}^c$ is reported in Fig. 5. The in-plane scaling predictions are constants lines – the asymptotes of more realistic space-scaling results. The GPS and (h_0, l) predictions turn out to be very similar, see Tables 1b, 1c.

A very slight decay of E_2^c is predicted by GPS as well as by the (h_0, l) method, cf. Fig. 6. Both models mentioned lead to very similar results, see Table 1d. The decay of E_2^c as well as of $\nu_{\alpha\beta}^c$ cannot be described within the framework of HASHIN'S [I.5] approach, hence the lack of comparisons.

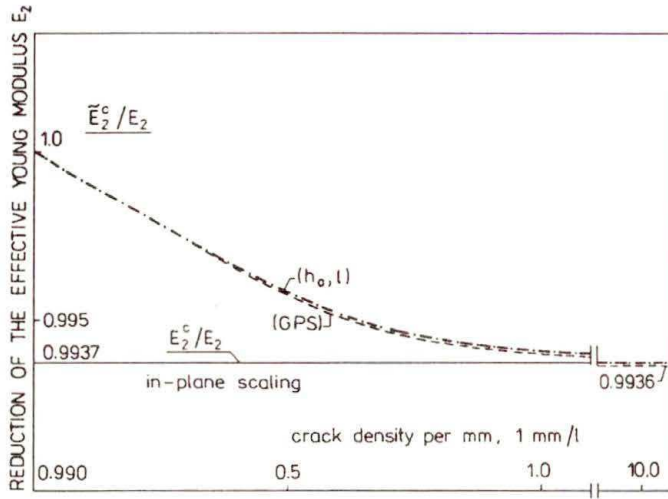


FIG. 6. The same laminate. Decay of the effective Young modulus E_2 .

The method of HASHIN [I.5] and the (h_0, l) method lead to the same formula describing the decay of the Kirchhoff modulus, cf. Fig. 7. Recently TSAI and DANIEL [I.16] have confirmed that this formula predicts values of G_{12}^c comparing favourably with experimental data concerning graphite/epoxy laminates, cf. Fig. 5

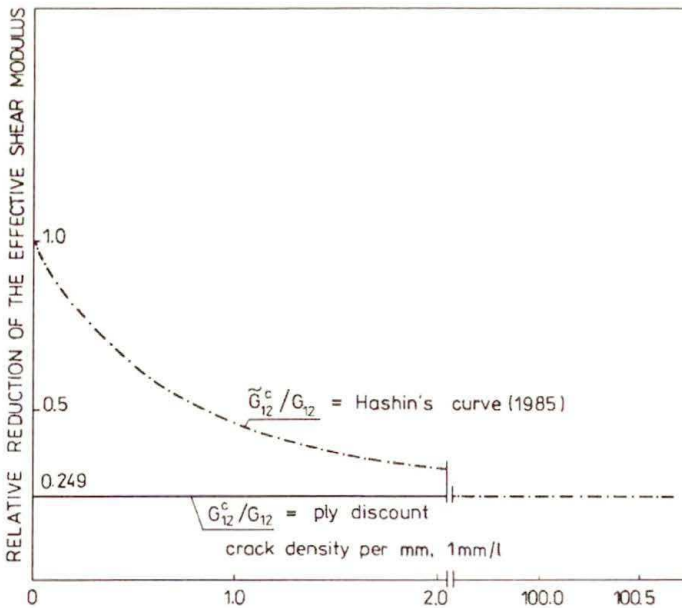


FIG. 7. The same laminate. Decay of the effective Kirchhoff modulus. The HASHIN'S [I.5] and (h_0, l) predictions coincide. Predictions based on the in-plane scaling coincide with ply-discount result.

in the cited paper. On the other hand, the experimental results due to HAN and HAHN [4] concerning the GFRP $[0_2^{\circ}, 90_2^{\circ}]_s$ laminates lie far away from the Hashin's curve. Experimental data concerning G_{12}^c for the laminate considered here were not available to the present authors.

3.2. $[0^{\circ}/90^{\circ}]_s$ glass/epoxy laminate

Consider the $[0^{\circ}/90^{\circ}]_s$ glass/epoxy laminate tested by OGIN *et al.* [9] for which

$$(3.5) \quad \begin{aligned} c = d = 0.125 \text{ mm}, \quad E_A = 40 \text{ GPa}, \quad E_T = 11 \text{ GPa}, \\ G_A = 5 \text{ GPa}, \quad G_T = 3.87 \text{ GPa}, \quad \nu_A = 0.3, \quad \nu_T = 0.42. \end{aligned}$$

These data, except for the last two which are assumed here, are taken from ABOUDI [1].

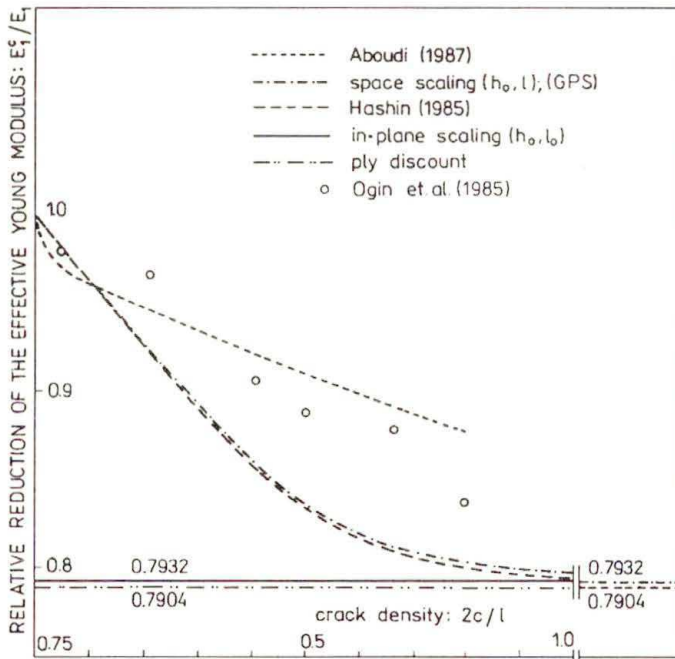


FIG. 8. The $[0^{\circ}/90^{\circ}]_s$ glass/epoxy laminate tested by OGIN *et al.* [9] (circles). Assessing the loss of the effective Young modulus E_1 .

The Hashin's curve as well as the almost coinciding curves provided by the GPS model of MCCARTNEY [I.12] and by the space-scaling (h_0, l) method yield lower bounds for the experimental results of OGIN *et al.* [9], cf. Fig. 8. The accuracy, however, is not so satisfactory as for the laminate considered previously. Better results are provided by the displacement-based method of ABOUDI [1]. His method, however, similarly to that of Hashin is based on comparing energies and hence is incapable of assessing off-diagonal terms of the effective stiffness matrix.

The precise values of E_α^c/E_α and $\nu_{\alpha\beta}^c$ predicted by the GPS model of MCCARTNEY [I.12, 13] and by the (h_0, l) model proposed in the present paper are set up in Tables 2a–2d. It is seen that both models produce almost identical results. In particular, these differences could not be displayed in Fig. 8 concerning E_1^c/E_1 .

Table 2. Decay of E_α^c/E_α , $\nu_{\alpha\beta}^c$ as function of crack density $2c/l$ for the $(0^\circ/90^\circ)_s$ glass/epoxy laminate tested by OGIN *et al.* (1985). Comparison of predictions by (h_0, l) model proposed and GPS approach of MCCARTNEY (1992, 1993).

(a)			(c)		
$2c/l$	E_1^c/E_1		$2c/l$	ν_{21}^c	
	McCartney (1992) GPS	Lewiński and Telega (h_0, l)		McCartney (1992) GPS	Lewiński and Telega (h_0, l)
0.1	0.96195	0.96194	0.1	0.11773	0.11789
0.5	0.83782	0.83780	0.5	0.07964	0.08030
1.0	0.79856	0.79846	1.0	0.06759	0.06839
100.	0.79333	0.79322	100.	0.06599	0.06680

(b)			(d)		
$2c/l$	ν_{12}^c		$2c/l$	E_2^c/E_2	
	McCartney (1992) GPS	Lewiński and Telega (h_0, l)		McCartney (1992) GPS	Lewiński and Telega (h_0, l)
0.1	0.12224	0.12241	0.1	0.99876	0.99881
0.5	0.09448	0.09529	0.5	0.99394	0.99421
1.0	0.08397	0.08501	1.0	0.99212	0.99247
100.	0.08250	0.08356	100.	0.99186	0.99223

3.3. $[0^\circ/90_2^\circ]_s$ graphite/epoxy laminate

Let us consider the loss of Young modulus of the $[0^\circ, 90_2^\circ]_s$ graphite/epoxy laminate with the following characteristics

$$(3.6) \quad \begin{aligned} d &= 0.127 \text{ mm}, & c &= 2d, & E_A &= 144.8 \text{ GPa}, & E_T &= 9.6 \text{ GPa}, \\ G_A &= 4.8 \text{ GPa}, & G_T &= 3.29 \text{ GPa}, & \nu_A &= 0.31, & \nu_T &= 0.46. \end{aligned}$$

The experimental results of GROVES [I.4] lie between the curve of LEE *et al.* [6] and the curve of HASHIN [I.5]; the curves (almost coinciding) provided by the GPS model and the space-scaling (h_0, l) approach lie slightly over the latter one, but all three curves are so close to each other that practically they overlap, cf. Fig. 9 and Table 3a. As in other cases, the in-plane scaling method leads to a line $E_1^c = 0.8842$ being an asymptote for the space – scaling curve. The Hashin's curve tends to the value 0.8840.

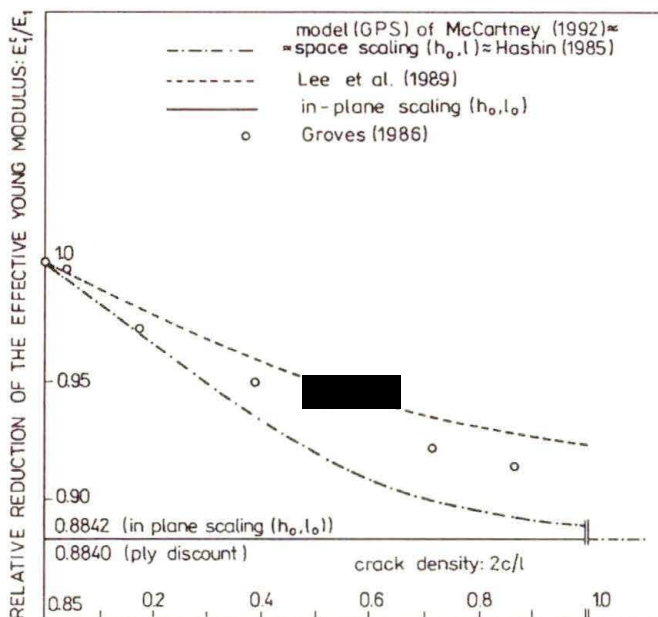


FIG. 9. The $[0^\circ/90^\circ]_s$ graphite/epoxy laminate tested by GROVES [I.4] (circles). Assessing the loss of the effective Young modulus E_1 .

Table 3. Decay of E_α^c/E_α , $\nu_{\alpha\beta}^c$ as function of crack density $2c/l$ for the $(0^\circ/90^\circ)_s$ glass/epoxy laminate tested by GROVES *et al.* (1986). Comparison of predictions by (h_0, l) model proposed and GPS approach of MCCARTNEY (1992, 1993).

(a)			(c)		
$2c/l$	E_1^c/E_1		$2c/l$	ν_{21}^c	
	McCartney (1992) GPS	Lewiński and Telega (h_0, l)		McCartney (1992) GPS	Lewiński and Telega (h_0, l)
0.1	0.98269	0.98270	0.1	0.02688	0.02689
0.5	0.91971	0.91973	0.5	0.01609	0.01614
1.0	0.88964	0.88964	1.0	0.01094	0.01101
100.	0.88418	0.88418	100.	0.01001	0.01001

(b)			(d)		
$2c/l$	ν_{12}^c		$2c/l$	E_2^c/E_2	
	McCartney (1992) GPS	Lewiński and Telega (h_0, l)		McCartney (1992) GPS	Lewiński and Telega (h_0, l)
0.1	0.04986	0.04988	0.1	0.99936	0.99936
0.5	0.03182	0.03192	0.5	0.99683	0.99685
1.0	0.02234	0.02248	1.0	0.99550	0.99553
100.	0.02055	0.02069	100.	0.99525	0.99528

The precise values of E_α^c/E_α and $\nu_{\alpha\beta}^c$ predicted by the GPS model of MCCARTNEY [I.12, I.13] and by the (h_0, l) one are given in Tables 3a–3d. The results are almost identical.

4. Final remarks

The analysis of the response of the cracked $[0_m^\circ, 90_n^\circ]$ laminates did not encompass a stress analysis. A detailed stress analysis will be published separately. We put only some relevant remarks concerning relations between (h_0, l) stress predictions and those found in HASHIN [I.5].

Within the framework of the (h_0, l) approach, the stresses in periodicity cells are expressed in terms of macrodeformations $\varepsilon_{\alpha\beta}^h$, cf. Eqs. (2.7)–(2.9) of [I.9] and (5.19)–(5.21) of [I.10]. On the other hand, in HASHIN [I.5] the stresses are determined by the density of the boundary shearing τ and tensile σ loading. To bridge a gap between both approaches let us introduce the following interpretations of τ and σ in terms of macro-stress resultants of the (h_0, l) model:

$$(4.1) \quad \tau = \tau_h = N_h^{12}/2h, \quad \sigma = \sigma_h = N_h^{11}/2h.$$

Let us focus our attention on the stresses arising at shear. According to (I.4.43) one finds

$$(4.2) \quad \tau_h = 2G_A \left[1 - F_{12}(\widehat{\lambda}\varrho) \right] \varepsilon_{12}^h.$$

Note that within the interpretation suggested by (4.1), τ_h becomes crack-density dependent: $\tau_h = \tau_h(\varrho)$. A direct relation links τ_h and ε_{12}^h , owing to which one can compare formulae for $\sigma_m^{12} = \sigma^{12}(x, z)$, $|z| < c$, due to HASHIN [I.5] with those resulting from the (h_0, l) model.

Using Eqs. (2.7) of [I.9] and (I.4.31) one finds

$$(4.3) \quad \sigma_m^{12}/\tau_0 = S_{12}^m(\widehat{\lambda}\varrho, \widehat{\lambda}\xi),$$

where $\tau_0 = 2G_A\varepsilon_{12}^h$ stands for the shear stress in the uncracked laminate and

$$(4.4) \quad S_{12}^m(x, y) = \frac{x(\operatorname{ch} x - \operatorname{ch} y)}{\frac{c}{d}\operatorname{sh} x + x \operatorname{ch} x}.$$

Note that τ_0 does not explicitly depend upon the crack density.

HASHIN [I.5] obtained the following relation

$$(4.5) \quad \sigma_m^{12}/\tau = 1 - \frac{\operatorname{ch} \widehat{\lambda}\xi}{\operatorname{ch} \widehat{\lambda}\varrho}.$$

Taking into account (I.4.42)₂ and (4.1) one can readily prove that formulae (4.3) and (4.5) coincide. Similarly, one can show that other components of the state of stress appearing when the laminate is subjected to shearing are predicted in the same manner by both models, inasmuch as a “bridging” relation (4.1) is acceptable.

Comparison of the formulae for stresses related to tension is less clear, since in general $N_h^{22} \neq 0$ while in HASHIN [I.5] only the case $N_h^{22} = 0$ (according to our interpretation) is considered. On imposing $N_h^{22} = 0$ one can derive a formula for $\sigma_m^{11} = \sigma^{11}(x, z)$, $|z| < c$:

$$(4.6) \quad \sigma_m^{11}/\sigma_h = f(\varrho, \xi),$$

where $\sigma_h = \sigma_h(\varrho)$, cf. (4.1)₂. HASHIN [I.5] normalized the stress σ_m^{11} with respect to the averaged stress in the middle layer. This formula does not coincide with (4.6) even if the latter is appropriately rearranged. For the laminate considered in Sec. 3.1, formula (4.6) produces results somewhat greater than its counterpart found by HASHIN [I.5], but the differences are measured in promilles.

The formulae found in the present paper for the decay of the effective stiffnesses and possible to find (but not displayed) formulae for stresses due to tension are more complicated than those found by HASHIN [I.5] and McCARTNEY [I.12, model GPS]. This is a consequence of treating the stress resultants $N^{\alpha\beta}$ as independent unknown variables and completion of the model with displacements v_α relevant to them. Note, however, that an independent treatment of $N^{\alpha\beta}$ is in general indispensable when the shapes of the laminate is arbitrary and $N^{\alpha\beta}$ cannot be determined directly by the boundary loading.

Thus the present paper does not present any set of formulae for the analysis of cracked laminates, but forms a consistent and well-posed laminate model (h_0, l) from which such formulae can be inferred. This model makes it possible to approximate boundary value problems for a relatively large class. It seems that the model constitutes a reasonable starting point to the construction of a damage model that would take into account:

- i) damage induced anisotropy, and ii) unilateral effect of damage.

According to CHABOCHE [3], none of hitherto existing theories of damage of laminates satisfies both the conditions simultaneously.

Acknowledgement

The authors were supported by the State Committee for Scientific Research through the grant No 3 P404 013 06.

References

1. J. ABOUDI, *Stiffness reduction of cracked solids*, Engng. Fract. Mech., **26**, 637–650, 1987.
2. D. ALLEN, C.E. HARRIS and S.E. GROVES, *A thermomechanical constitutive theory for elastic composites with distributed damage. Part I. Theoretical development. Part II. Application to matrix cracking in laminated composites*, Int. J. Solids Struct., **23**, 1301–1318; 1319–1338, 1987.
3. J.-L. CHABOCHE, *Damage induced anisotropy: on the difficulties associated with the active/passive unilateral condition*, Int. J. Damage Mech., **1**, 148–171, 1992.
4. Y.M. HAN and H.T. HAHN, *Ply cracking and property degradations of symmetric balanced laminates under general in-plane loading*, Compos. Sci. Technol., **35**, 377–397, 1989.
5. Z. HASHIN, *Analysis of orthogonally cracked laminates under tension*, J. Appl. Mech. Trans. ASME, **54**, 872–879, 1987.
6. J.-W. LEE, D.H. ALLEN and C.E. HARRIS, *Internal state variable approach for predicting stiffness reductions in fibrous laminated composites with matrix cracks*, J. Compos. Mater., **23**, 1273–1291, 1989.
7. T. LEWIŃSKI and J.J. TELEGA, *Stiffness loss of laminates with aligned intralaminar cracks. Part I. Macroscopic constitutive relations*, Arch. Mech., **48**, 2, 245–264, 1996.
8. S. MOTOGI and T. FUKUDA, *Shear modulus degradation in composite laminates with matrix cracks*, [in:] Proc. Mechanical Behaviour of Materials-VI, M. JONO and T. INOUE [Eds.], Pergamon Press, Oxford, pp. 357–362, 1991.
9. S.L. OGIN, P.A. SMITH and P.W.R. BEAUMONT, *Matrix cracking reduction during the fatigue of a (0°/90°)_s GFRP laminate*, Compos. Sci. Technol., **22**, 23–31, 1985.
10. P.A. SMITH and J.R. WOOD, *Poisson's ratio as a damage parameter in the static tensile loading of simple crossply laminates*, Compos. Sci. Technol., **38**, 85–93, 1990.

WARSAW UNIVERSITY OF TECHNOLOGY
CIVIL ENGINEERING FACULTY
INSTITUTE OF STRUCTURAL MECHANICS
and
POLISH ACADEMY OF SCIENCES
INSTITUTE OF FUNDAMENTAL TECHNOLOGICAL RESEARCH.

Received June 21, 1995.